Site specific SEM/FIB/TEM for analysis of lubricated sliding wear of aluminium alloy composites

JC Walker, H Jones and WM Rainforth

Department of Engineering Materials, University of Sheffield, Sheffield, S1 3JD UK.

m.rainforth@sheffield.ac.uk

Abstract. Although extensive research has been undertaken into the dry sliding wear of aluminium alloys, only limited work has been reported on the lubricated wear. In this paper, the lubricated sliding wear of some powder derived aluminium alloy composites is reported. Stereo pairs of the worn surface were obtained in the SEM and digitally reconstructed to give a quantitative projection of the surface topography. Analysis of the average surface roughness (Ra) along chosen sections provided quantitative information about the wear mechanism. Following this, dual beam focused ion beam (FIB) was undertaken to further explore the features revealed by the SEM surface reconstructions, with TEM sections removed from selected regions. Surface deformation was confined to a narrow layer, typically 1μm thick. Subgrain size within the subsurface layer was comparable to that found in dry sliding wear tests. Reinforcement fracture occurred in the surface particles only. The resultant fragments were often incorporated back into the surface following detachment, such that the total volume fraction reinforcement at the surface was greater than in the bulk. Thus, the dynamic surface topography was a result of three factors: surface deformation, local detachment of reinforcement and re-incorporation of the fragments back into the surface.

1. Introduction

The use of aluminium alloys and composites for sliding contact surfaces has been extensively investigated in an effort to optimise the material properties for wear resistance [1]. Although there have been many studies on the effect of material and test parameters, relatively few pertain to the lubricated sliding of these materials, perhaps surprising given that this is the industrially relevant condition.

In an effort to understand the effect of lubricated sliding on the near surface layer of aluminium alloy composites, a number of powder metallurgy/extruded composites were wear tested under lubricated sliding conditions and the worn surfaces characterised using SEM/FIB/TEM.

2. Experimental Procedure

AA2124 and AA5056 were blended with either SiC, Cr_3Si, or $MoSi_2$ and hot extruded (450ºC), such that a nominally 15vol.% volume fraction reinforcement was obtained. Extrusions of the unreinforced alloys were also carried out under the same parameters for comparison. The resulting composites were sectioned in the transverse plane and polished to <0.1μm R_a, prior to wear testing in a pin-on-ring configuration against a hardened (705H_v) M2 tool steel counterface, also polished to <0.2μm R_a.

A high normal load (630N) was applied via a cantilever beam, which allowed initial Hertzian point contact stresses in the range 0.9-1.2GPa, according to the elastic properties of each material. Lubricated sliding was achieved by partially immersing the counterface in an oil bath of Mobil 1 Motorsport 15W-50, with tests run at $1ms^{-1}$ for distances of hundreds of kilometres to assess the wear response over extended sliding distances.

SEM observations of the worn surface were carried out using a Jeol 6500Fabrika. Secondary electron stereo pairs of the worn surfaces were obtained by tilting the images 16º apart at magnifications of >x1000. Mex software, from Alicona, allowed digital reconstruction of the worn surface topography, providing a 3-dimensional visualisation of the worn surfaces. Profile traces of 100 pixel width were taken perpendicular to the wear direction and provided quantitative information about the local surface roughness.

Dual beam focused ion beam (FIB, Jeol 6500Fabrika; 30kV and 1.5μA) allowed site specific investigation of subsurface areas by milling sections parallel to the worn surface Secondary ion imaging made use of the ion channelling contrast effect to provide information about grain orientations.

TEM samples were prepared from selected regions by both lift-out and trench techniques. Surfaces were protected by either deposition of Pt or W from a metal precursor gas, or in the case of the trench technique, as applied to 5056 alloy, by Ni plating using Electroless Nickelmerse, followed by sectioning and grinding to ~30μm thickness, prior to FIB thinning. TEM observations of the worn surfaces were carried out using a FEI Tecnai operating at 200kV.

3. Results and Discussion

3.1. Specific Wear Rates

Figure 1 shows the relative wear rates of the unreinforced alloys to be significantly higher than the reinforced composites, as expected. It would appear that the harder precipitation strengthened alloy 2124 (119.6H_v) is more wear resistant than the softer 5056 work hardening alloy (95.8H_v). Alloys reinforced with intermetallics all showed a decrease in the relative wear rates compared to the alloys, with silicide reinforced composites showing similar or lower wear rates compared to a more traditional SiC reinforced composite.

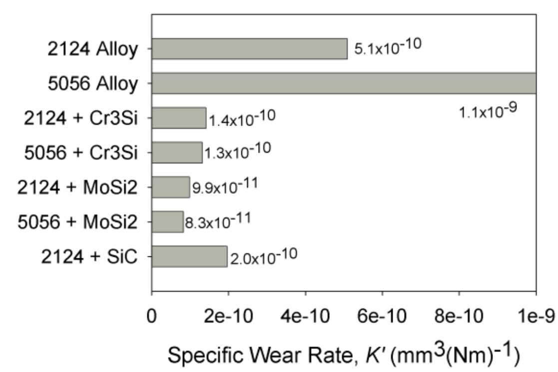

Figure 1. Specific wear rates for lubricated sliding wear of Al alloys and composites.

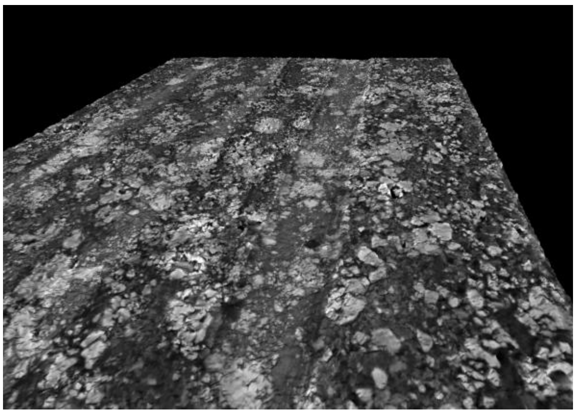

Figure 2. 3-D surface reconstruction of the worn surface 2124 + $MoSi_2$, x1000.

3.2. SEM Observations

SEM analysis of the worn surface of unreinforced alloys indicated a surface characterised by both broad (10µm) and narrow (<1µm) wear tracks, along with a multitude of craters and smaller wear debris particles from the counterface. 3-D stereo reconstructions of areas where transfer of particles from the counterface to the alloy had taken place indicated that the particles were flush to the surface, evidence of the high contact pressure exerted from the counterface and the plastic yielding of the matrix to accommodate them.

Observations of the response of the composite surfaces to lubricated sliding differed according to type of reinforcement. In the case of silicide reinforced alloys, a relatively polished surface was observed, Figure 2, with extensive fracture of the reinforcement appearing to cause an increase in the local surface volume fraction. As previously reported [2] this was indeed the case with volume fractions increasing from 15vol.% to ~25vol.% for 2124 reinforced composites and to ~35vol.% for 5056 composites.

In the case of 2124 + SiC the 3-D model showed a small (~3.5µm) distribution in asperity heights however, the abrasive 3rd body effect of the SiC particles resulted in a much rougher composite surface topography, as indicated by profile traces perpendicular to the wear tracks. R_a values calculated from the primary profiles indicated that the smoothest worn surface was for the 5056 alloy (R_a=0.10µm, 0.12µm), whilst 2124 + SiC was the roughest (R_a=0.20µm, 0.17µm), as expected. However these values of surface roughness are still relatively low, given that an average metallographic polish can also yield similar values [3]. The metallographic evidence therefore indicates that at extended sliding distances the alloys and composites were operating in the 'mild wear regime', with fine-scale abrasion by second and third bodies the main material removal mechanism.

Table 1. Average roughness values (R_a) of worn surfaces.

	Roughness, Ra (µm)
5056 Alloy; Area 1	0.101
5056 Alloy; Area 2	0.126
5056 + 15vol.% MoSi2	0.138
2124 + 15vol.% MoSi2	0.159
2124 + 15vol.& SiC; Area 1	0.203
2124 + 15vol.& SiC; Area 2	0.174

3.3. Focused ion beam

Ion channelling contrast of sub-surface sections revealed a near surface layer of heavy plastic deformation, approximately 1µm deep for all samples investigated, except 2124 + SiC. The strain of features, e.g. small particles and grain boundaries towards the sliding direction was evident, as was the nucleation of sub-surface voids, giving further evidence of the high levels of local contact stress applied [2].

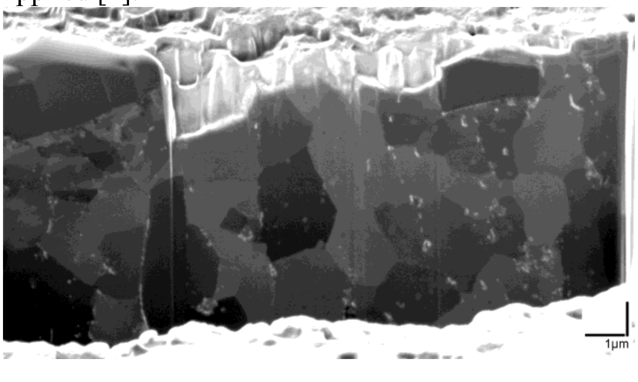

Figure 3. Focused ion beam milled section from the worn surface 2124 + 15vol.% SiC composite, parallel to the sliding direction

In the case of 2124+ SiC, however, this surface deformed layer was not present. Instead, relatively equiaxed grains, approximately 2µm in size, were observed near the worn surface, Figure 3. However, sub-surface deformation was observed at depths greater than 1µm below second phase reinforcing particles, where the reinforcement was slightly proud of the surface. This demonstrates that the high points acted as the contacting asperities, and load transfer occurred at these points from the reinforcement to the subsurface matrix. Importantly, the nearby angular pits were a result of loss of the SiC via fracture of the reinforcement/matrix interface, resulting in the liberation of hard ceramics as 3rd body abrasives. This would indicate why 3-D surface reconstructions show a high roughness for the topography of the aluminium alloy-SiC composite, which is fully consistent with the observation that the counterface to these composites suffers from abrasive wear.

3.4. Transmission electron microscopy

TEM observations of the worn surface of the unreinforced 5056 alloy, Figure 4, indicated that the region of heaviest plastic deformation, whilst confined to approximately 1µm below the worn surface, was similar to that seen for dry sliding of aluminium against steel [4]. Sub-grain sizes as low as 30nm were seen in dark-field images of material believed to be debris particles that had adhered to the worn surface. Average grain sizes of the bulk material as the surface was approached were of the order 90nm in heavily deformed regions, with selected area diffraction pattern from the near surface confirming the polycrystalline nature.

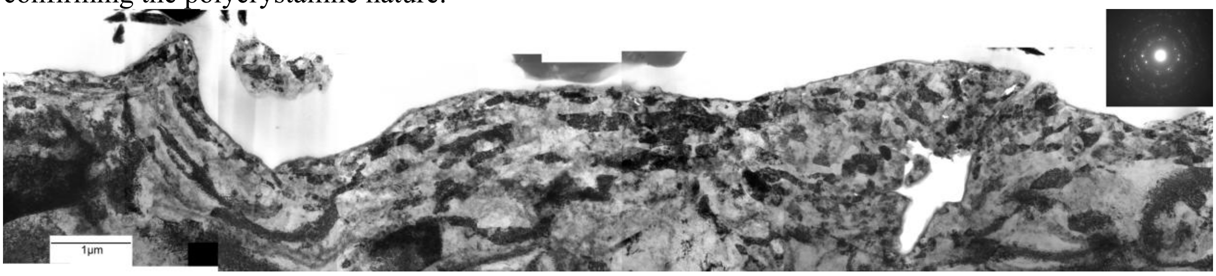

Figure 4. FIB thinned TEM cross-section of the worn 5056 alloy surface.

4. Summary

The dynamic surface topography and its influence on the wear mechanism associated with the lubricated sliding of these aluminium alloys and composites depended largely on the material properties, in particular the reinforcement type. Unreinforced alloys were subjected to severe deformation of the near surface layer, to a level similar to that seen for dry sliding wear. Silicide reinforced composites exhibited an interesting ability to increase their surface volume fraction reinforcement through fracture and re-incorporation of the particles into the surface. This allowed wear rates, at an extended sliding distance, to be similar to that of a conventionally reinforced SiC composite. SiC reinforcements are effective at transferring contact loads to the matrix, but at the same time are also prone to fracture at the particle/matrix interface. The 3rd body abrasive action of these particles leads to a much rougher surface topography, and the overall wear resistance becomes a compromise between the two competing beneficial and detrimental effects.

Acknowledgements

Grateful thanks are given to EPSRC for funding the studentship for this work.

References

[1] A.P. Sannino and H.J. Rack, Dry sliding wear of discontinuously reinforced aluminium composites: review and discussion, Wear 189 (1195) 1-19

[2] J.C.Walker, W.M. Rainforth, H.Jones, Lubricated sliding wear behaviour of aluminium alloy composites, Wear 259 (2005) 577-589

[3] K.J. Stout, Materials in Engineering, 2, 1981, 287-295

[4] C.Perrin and W.M.Rainforth, The effect of alumina fibre reinforcement on the wear of an Al-4.3%Cu alloy, Wear 181-183 (1) 312-324